Assessment of OLED displays for vision research

Emily A. Cooper Department of Psychology, Stanford University, Stanford, CA, USA

Haomiao Jiang Department of Electrical Engineering, Stanford University, Stanford, CA, USA

Vladimir Vildavski Department of Psychology, Stanford University, Stanford, CA, USA

Joyce E. Farrell Department of Electrical Engineering, Stanford University, Stanford, CA, USA

Anthony M. Norcia Department of Psychology, Stanford University, Stanford, CA, USA

Vision researchers rely on visual display technology for the presentation of stimuli to human and nonhuman observers. Verifying that the desired and displayed visual patterns match along dimensions such as luminance, spectrum, and spatial and temporal frequency is an essential part of developing controlled experiments. With cathode-ray tubes (CRTs) becoming virtually unavailable on the commercial market, it is useful to determine the characteristics of newly available displays based on organic light emitting diode (OLED) panels to determine how well they may serve to produce visual stimuli. This report describes a series of measurements summarizing the properties of images displayed on two commercially available OLED displays: the Sony Trimaster EL BVM-F250 and PVM-2541. The results show that the OLED displays have large contrast ratios, wide color gamuts, and precise, well-behaved temporal responses. Correct adjustment of the settings on both models produced luminance nonlinearities that were well predicted by a power function ("gamma correction"). Both displays have adjustable pixel independence and can be set to have little to no spatial pixel interactions. OLED displays appear to be a suitable, or even preferable, option for many vision research applications.

Introduction

Vision researchers often come up against the limits of displays when creating stimuli for visual experiments. Raster-scanned cathode-ray tubes (CRTs) have long been the preferred display technology for vision research, and the properties and potential pitfalls of these displays are well documented (Bach, Meigen, & Strasburger, 1997; Brainard, Pelli, & Robson, 2002; Cowan, 1995; García-Pérez & Peli, 2001; Lyons & Farrell, 1989; Sperling, 1971). In the past decade, liquid crystal displays (LCDs) have all but replaced CRTs in the consumer display market, making CRTs less readily available for lab research. While LCDs offer some advantages over CRTs—mainly, better spatial uniformity and pixel independence—their spectral and temporal properties make them inadequate for certain types of vision research (Elze & Tanner, 2012; Farrell, Ng, Ding, Larson, & Wandell, 2008; Pardo, Pérez, & Suero, 2004; Watson, 2010). Assessments of more recent LCD models demonstrate that advances in LCD technology have overcome some of these limitations (Kihara, Kawahara, & Takeda, 2010; Lagroix, Yanko, & Spalek, 2012).

Recently, display panels made with organic light emitting diodes (OLEDs) have become commercially available. These display panels are comprised of pixels that use an electrical circuit to control the emission of light from a thin film of organic electroluminescent material (see Geffroy, le Roy, & Prat, 2006, for review). OLED technology has many promising properties for vision research: self-emitting pixels, fast response times, wide color gamut, and high contrast. Recent full color, large display panels comprised of OLED pixels have

Citation: Cooper, E. A., Jiang, H., Vildavski, V., Farrell, J. E., & Norcia, A. M. (2013). Assessment of OLED displays for vision research. *Journal of Vision*, *13*(12):16, 1–12, http://www.journalofvision.org/content/13/12/16, doi:10.1167/13.12.16.

doi: 10.1167/13.12.16 Received June 17, 2013; published October 23, 2013 ISSN 1534-7362

overcome issues such as color lifetime and power consumption sufficiently well for commercial applications (Lee & Song, 2012; Lee et al., 2013; Singh, Narayanan Unni, & Solanki, 2012). However, the pros and cons of commercially available OLED display panels and drivers for vision research are not well known. The goal of the current report is to serve as an entry point for researchers interested in using OLED displays to create visual stimuli for experiments. We report measurements of the luminance, spectral, spatial, and temporal properties of two commercially available OLED displays. Another recent report (Ito, Ogawa, & Sunaga, 2013) describes the evaluation of the one of the models assessed here (Sony Trimaster EL PVM-2541). The present results corroborate and extend Ito et al.'s (2013) measurements on the PVM-2541 monitor and provide additional measurements for the Trimaster EL BVM-F250 model.

Methods

Displays

Assessments were performed on two Sony OLED models: the Trimaster EL BVM-F250 Master Monitor (BVM), a high-end professional video monitor for production applications, and the Trimaster EL PVM-2541 Picture Monitor (PVM), a video monitor designed for general usage (http://pro.sony.com/bbsc/ssr/cat-monitors/cat-oledmonitors/). The BVM model was controlled using the separate BKM-16R Monitor Control Unit; the PVM has controls built into the monitor. Both displays offer full HD resolution (1920 × 1080 pixels) and a 10-bit color driver and engine that work with certain video input formats. The displays have the same dimensions: 54.3 × 30.6 cm (62.3 cm diagonal). Pixels are 0.283 × 0.283 mm. As of publication, the two BVM and PVM series models that were assessed have been replaced with a next-generation set of displays, with identical model names with addition of the letter "A." These new models are described as having identical specifications to the previous generation, but with an improvement in off-axis viewing performance.

Computer software and hardware

For luminance, spectral, and pixel independence measurements, stimuli were generated using MATLAB (The MathWorks, Inc.) and Psychtoolbox-3 (Brainard, 1997; Kleiner, Brainard, & Pelli, 2007; Pelli, 1997) on a Mac Pro (mid-2010) running OSX (10.6.8). The computer was equipped with an ATI Radeon HD 4870 graphics card, the upgrade graphics card for the previous Mac Pro model (early-2009). This graphics card was used because it is compatible with the PsychToolbox-3 Mac OSX kernel driver (http://docs.psychtoolbox.org/PsychtoolboxKernelDriver). The Mac Pro was connected to the displays via the DVI port, using a DVI-to-HDMI adapter.

For temporal measurements, stimuli were created using a PowerBook G4 running OS9.2, compatible with the custom hardware required for these measurements, discussed below. The PowerBook was connected to the displays via a DVI-to-HDMI adapter.

Dynamic dithering versus 10-bit graphics

Initial measurements suggested that the displays' panel drivers and the software/hardware set up described here were compatible with the Psychtoolbox-3 (3.0.10) kernel driver for Apple OSX, enabling the display of 10-bits per color channel. After additional measurements, it was determined that the graphics card was not outputting a genuine 10-bit signal, but instead the output was an 8-bit dithered version of the 10-bit signal being generated with MATLAB and Psychtoolbox. However, the specific ATI graphics card used here (Radeon HD 4870) employs dynamic spatio-temporal dithering that sacrifices little spatial resolution, and which provides measurably distinct local light intensity values at a resolution above 8-bits. The luminance values reported here are the output of this dithering method. That is, we created stimuli in MATLAB in 10-bit steps (1024 luminance values) and sent these to the graphics card for conversion to an 8-bit dithered signal. We will refer to these input values as "bit values."

The manufacturer documentation indicates that these displays are compatible with 10-bit graphics pipelines with certain video input formats. However, in the current report their compatibility with standard vision research set ups, including HDMI video input, was not verified.

Luminance

Luminance measurements were taken using a PIN-10AP photodiode with a v-lamda photometric filter providing input to a custom hardware signal conditioning unit (LightMouse). The unit was connected by USB to a PowerBook G4 running OS9.2 and custom registration software (PowerDiva). The absolute luminance of the measurements was calibrated and corrected for a slight gain offset using a PhotoResearch PR715 photometer (http://www.photoresearch.com/current/pr705.asp). At the start of each measurement, the dark level of the photodiode was noted and subtracted from the results. The photodiode has high

sensitivity at low luminance, and the ability to reliably detect luminance as low as 0.01 cd/m^2. The measurements were taken from the center of the monitors at each of the 1024 bit values with full screen illumination of all subpixel components (white). As a screen uniformity test, additional measurements were taken at 128-bit values in the upper left corners of the monitors, as well as in the monitor center with only half-screen illumination. Manufacturer-default brightness (black level) and contrast settings were used for the BVM (zero and 1,000, respectively). Initial measurements indicated that the recommended contrast setting on the PVM lead to saturation in the upper luminance range (See Ito et al., 2013, for a detailed description of the saturation effect). To correct this, the display contrast setting was reduced from 80 to 70, and the brightness was left at the default 50. All measurements were collected with these altered settings. Both displays offered several options for luminance nonlinearity ("gamma correction"). A gamma correction setting of 2.2 was used, indicating a luminance nonlinearity that should follow a power function with an exponent of 2.2. Each set of measurements was fit with a power function to estimate the accuracy of the manufacturer gamma correction.

Spectrum

Spectral measurements were taken using the displays' native and SMPTE (Society of Motion Picture and Television Engineers) color modes, the Photo-Research PR715 photometer and the VistaLab calibration routine (http://vistalab.stanford.edu/trac/pdcsoft/browser/trunk/Devices/PR715?rev=26). The energy spectra of the red, green, and blue subpixel components were measured separately at 100% luminance in steps of 4 nm. Measurements were repeated with all subpixel components simultaneously to assess spectral additivity—whether the spectrum of white is a linear combination of the individual components (Brainard, 1989). Maximum luminance was measured at the center of the screen separately for each subpixel component to assess the relative luminance of each color component. Display color gamuts in terms of X- and Y-chromaticity were assessed in the native and SMPTE color modes. All gamuts were calculated and plotted using the Vset Toolbox for Matlab (https://github.com/hhiro/HumanTrichromacyRevisited2012/tree/master/vsetToolBox).

Pixel independence

Pixel independence measurements were taken to assess the additivity of two horizontally adjacent pixels and two vertically adjacent pixels. Each pixel was illuminated to 60% of its maximum luminance. Pixels were imaged separately and simultaneously using a Nikon D2Xs digital camera with custom lens and light baffle (Farrell et al., 2008). The lens and baffle enabled imaging of pixels with a magnification factor of 20. Images were saved in the raw Nikon image format (NEF) and compared using MATLAB and the dcraw package (http://www.cybercom.net/~dcoffin/dcraw/). To test for pixel interactions (spatial additivity), the red, green, and blue values of linear camera images of the two single pixels were summed together and compared to the simultaneous image. If the adjacent pixels add linearly, the summed image will be equivalent to the simultaneous image (Farrell et al., 2008).

Both displays have the option to use an *aperture correction* parameter to enhance image edges (Hagerman, 1993). Aperture correction is a parameter for edge enhancement and blurring in Sony OLED displays and, contrary to convention, it does not refer to aperture settings for cameras. To assess the effect of edge enhancement and blurring, pixel independence measurements were taken with and without this feature.

Temporal precision

Temporal measurements were taken with a linear silicon photodiode conditioned to provide an analog voltage output which was digitized at a 1560 Hz sampling rate by a custom data acquisition system (PowerDiva). The software displayed images alternating at 5 Hz and 30 Hz between 97.5% and 2.5% of the maximum luminance. Voltages were converted to candelas-per-square meter (cd/m^2) units using the luminance measurements described above. Both the BVM and PVM monitors were tested with refresh rates set to 60 Hz, the maximum available. The PVM model was also measured with the "flicker free" option enabled. For comparison, the same measurements were repeated on two LCDs (Dell U2410 and LG Flatron D2342) and a CRT (HP P1230). Both LCDs were also connected to the PowerBook via a DVI-to-HDMI adapter; the CRT was connected with a VGA cable. The Mac OSX Displays software included 24 and 25 Hz refresh rate options for both OLED displays. To verify these refresh rates, measurements were taken with a static screen.

Results

Luminance

Figure 1 shows the luminance values in cd/m^2 for each bit value measured at the center of the screen with

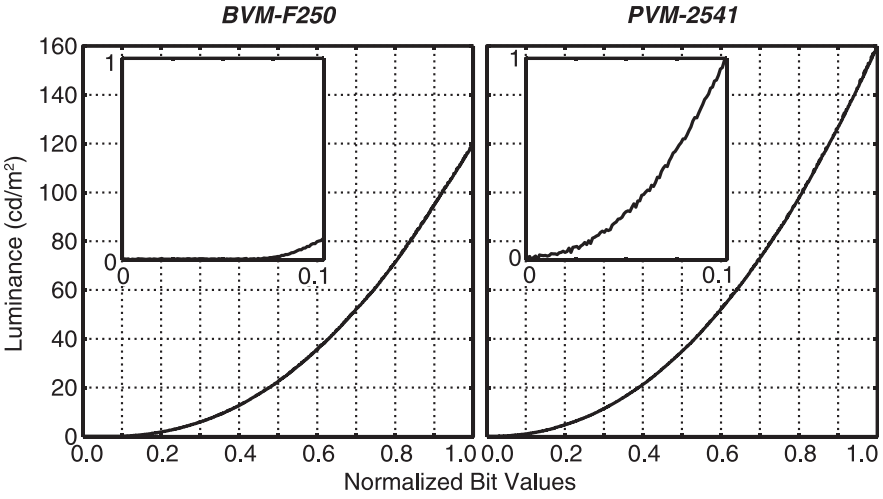

Figure 1. Luminance profiles of the BVM and PVM OLED displays. Abscissa values indicate normalized (0 - 1) bit values. Ordinate values indicate luminance measured by the photodiode in candelas per square meter. Insets show magnified view of the lowest 10% of the bit values.

the full screen uniformly illuminated. Table 1 contains a summary of several of the measured luminance properties under these conditions. The maximum luminance was greater on the PVM than the BVM by ~30% with the tested display settings. Minimum luminance values reported are the lowest luminance values that were reliably detected by the photodiode. In the case of both displays, some number of the lowest bit values produced luminance levels that were too dark to measure (75 values for the BVM and 12 values for the PVM), so the reported minimum luminance reflects the luminance measured at the 76th and 13th bit values, respectively. The insets of Figure 1 show a magnified view of the lowest 102 bit values, making this floor effect visible. In both cases, the first detectable luminance value matched the photodiode's sensitivity (0.01 cd/m^2). Because the OLED display panels have self-emitting pixels, the true minimum luminance is theoretically 0 cd/m^2. But for the purposes of display calibration it is useful to determine the bit value at which the minimum measureable luminance occurs. The contrast ratio reported is the ratio between the maximum and minimum luminance. These measurements depend greatly on the display settings, so they should just serve as an example of the luminance and contrast properties of the displays.

To determine the accuracy of the gamma correction (predicted to be a power function with an exponent of 2.2) on both displays, the luminance measurements were replotted on a logarithmic scale along with the predicted power function. On a logarithmic scale, a power function is linear. Deviations in the data from the slope of the prediction would indicate that the exponent of the power function is not exactly 2.2; deviations in the data from linearity would indicate that the luminance nonlinearity of the displays is not well fit by a power function. Figure 2 shows the data in this format. The left-most panel shows the results using the default brightness and contrast setting on the BVM (those also plotted in the left panel of Figure 1). Luminance measurements (a subset) are normalized and plotted as black circles, and the predicted power function is plotted as a gray line. The noise floor of the photodiode is visible in the noisy measurements below a normalized luminance of 10^{-4}. Beyond that noise floor, the data are clearly not linear, indicating that a power function is not a good approximation of the display's luminance nonlinearity. The central panel shows luminance values from the BVM when the display brightness (black level) was increased from the default (brightness was set to 50 instead of zero and luminance was remeasured at 32 of the bit values). With these altered settings, the luminance nonlinearity was well fit by a power function, with a best-fit power of 2.2 and a square root of the mean squared difference (RMSD) between the data and the prediction of 0.8 cd/m^2. The right-most panel shows the data for the PVM (which notably had the contrast setting reduced from default to avoid luminance saturation, as described in the Methods), which are also well fit by a gamma power of 2.2 (RMSD = 0.2 cd/m^2). This suggests that in some circumstances, the brightness and

	BVM-F250	PVM-2541
Maximum luminance (cd/m^2)	119.6	159.4
Minimum luminance (cd/m^2)	0.01	0.01
Measured contrast ratio	11,960 : 1	15,940 : 1

Table 1. Summary of the luminance properties of each display using the default settings (except the PVM contrast).

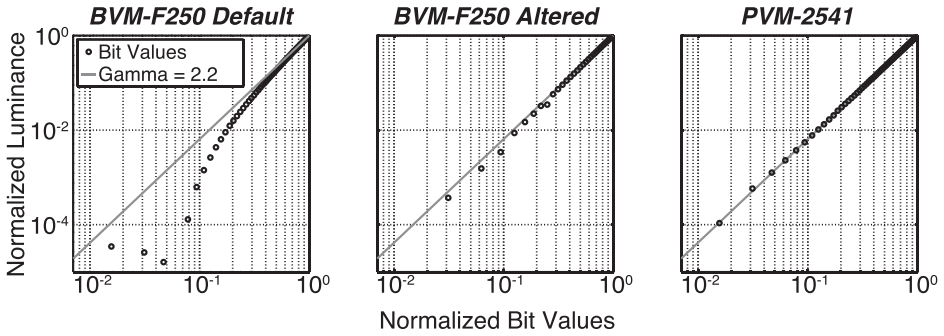

Figure 2. Luminance profiles of the BVM and PVM OLED displays as compared to the gamma correction setting. Abscissa values indicate normalized (0 - 1) bit values. Ordinate values indicate normalized luminance. Gray lines show predicted luminance for the gamma correction used during the measurements (a power function with an exponent of 2.2). In the left and right panels, a subset of the data from Figure 1 are plotted as black circles; these luminance values were measured by the photodiode in candelas-per-square meter and the normalized to a scale of 0-1. In the central panel, 32 new measurements from the BVM (after increasing the display black-level) are plotted.

contrast settings of the display may interact with its actual gamma correction, or may cause floor or saturation effects at the lowest and highest bit values (See Ito et al., 2013, for additional analysis of display settings and saturation). Care should be taken in measuring the luminance values for a specific combination of display settings if one wants to undo the luminance nonlinearity for experimental purposes ("linearize" the display).

Measurements taken in the upper left corner of the displays had an RMSD from the center-screen measurements of 1.0 cd/m^2 on the BVM and 1.2 cd/m^2 on the PVM. Measurements taken with half-screen illumination had an RMSD from full screen illumination of 0.1 cd/m^2 on the BVM and 0.2 cd/m^2 on the PVM. This result, however, was contingent on not overpowering the display. That is, for some combinations of brightness and contrast, the luminance would saturate, and that saturation occurred at different bit values depending on the percentage of the screen being illuminated.

In Ito et al.'s (2013) assessment of the PVM model, the luminance and spatial uniformity measured with comparable display settings were in good agreement with those reported here (results for additional brightness/contrast settings were also reported). Using a different photometer (Konica Minolta CS2000), the authors measured a minimum luminance below 4×10^{-5} cd/m^2, well below the level detectable by the human eye in a dark room. This is consistent with our assessment that the minimum luminance of the OLED panels is likely below the noise floor of most common photometric devices.

Spectrum

Figure 3 shows the spectral energy for each display in the native color mode at the maximum luminance. Red, green, and blue lines indicate the energy spectra of the red, green, and blue subpixels, respectively. Table 2 reports the maximum luminance of each individual color component, the sum of these values, and the difference relative to the maximum luminance of white. The difference is small, indicating that the subpixels are close to linearly additive—the white spectrum is equal to the sum of the individual spectra.

Figure 4 shows the color gamut of each display in CIE *xy* space. The full color spectrum locus is shown as a solid line. The chromaticity coordinates of the three color subpixels are plotted a circles and connected by straight lines to illustrate the displayable gamut. The color gamut for the native color mode is shown by the dashed line. The SMPTE color mode is shown by the dotted line. The native gamuts of the BVM and PVM exceed the SMPTE gamut for the red, green, and blue stimuli, indicating that the color gamut of both OLEDs exceeds that of a typical CRT. This can be attributed to the color purity of the light emitted by the electroluminescent materials used to create the red, green, and blue subpixel components of the OLED panels. Chromaticity *xy* coordinates for each subpixel in the native color modes are reported in Table 3. For the PVM, these coordinates are in good agreement with the previous report (Ito et al., 2013).

Pixel independence

Figure 5 illustrates the method of testing pixel independence. For these tests, two images are compared: a *composite* image created by linearly summing images captured of two vertically or horizontally adjacent pixels individually (upper panel) and a *simultaneous* image created by capturing both pixels illuminated at once (lower panel).

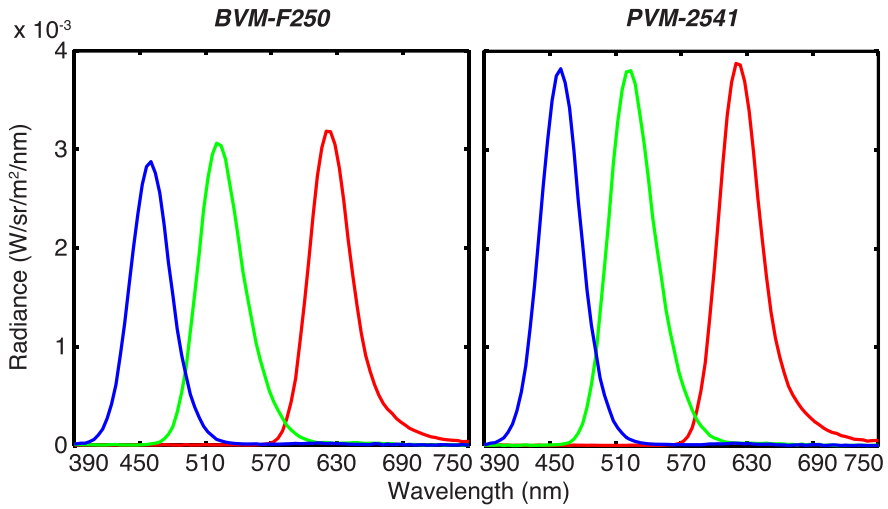

Figure 3. Spectral profiles of the BVM and PVM OLED displays in native color mode. Abscissa values indicate wavelength in nanometers. Ordinate values indicate radiance measured by the PhotoResearch PR 715 photometer in watts per steradian per square meter per nanometer. Each line color represents the subpixel components: red, green, and blue.

Figure 6 shows the results of the pixel independence tests for each display. Red, green, and blue channels from the raw Nikon camera images are plotted separately. If the pixels are spatially independent, the composite image should be a good predictor of the simultaneous image and therefore the red, green, and blue data should fall near the identity line. For each display, results for horizontally and vertically offset pixels are shown in separate columns. Each row shows the results for a different display aperture setting. *Aperture* refers to edge enhancement/blurring operations performed by the display. On the BVM, there are 201 possible aperture values (0–200) and three examples are shown: zero, 50, and 100. On the PVM, there are seven possible aperture values (0–6) and four examples are shown: zero, three, four, and six.

Table 4 summarizes the agreement between simultaneous and composite images for each of the edge enhancement/blurring settings (aperture). Each set of data was fit with a linear regression. Slopes of the best-fit lines (averaged across color components) are reported. Changing the aperture settings only affected the interactions between horizontally adjacent pixels. Slopes of one (indicative of good pixel independence) occur for horizontally adjacent pixels when aperture is set to zero on the BVM and to four on the PVM, as well as for vertically adjacent pixels on the BVM regardless of aperture.

Slopes less than one indicate that the simultaneous image was darker than predicted by the composite. This pixel interaction reflects the action of the edge enhancement: it boosts the high spatial frequencies of the image and increases the intensity of individual pixels (composite) more than the intensity of the two adjacent pixels (simultaneous). This occurs for horizontally adjacent pixels when aperture is set above zero on the BVM and above four on the PVM. Slopes greater than one indicate that the simultaneous image was brighter than predicted. This pixel interaction reflects the edge blurring action of aperture: the blurring dampens the high spatial frequencies of the image and lowers the intensity of individual bright pixels surrounded by the black background (composite) more than the intensity of the two adjacent pixels (simultaneous). This occurs only on the PVM for horizontally adjacent pixels when aperture is set below four and for vertically adjacent pixels at all aperture settings.

These results show that near-perfect pixel independence can be achieved on the BVM if edge enhancement is disabled by setting aperture to zero. On the PVM, horizontal pixel independence is achieved with an aperture setting of four; however, with all settings there is an edge blurring interaction between vertically adjacent pixels. Ito et al. (2013) assessed pixel interactions on the PVM by measuring the average luminance of vertical lines, horizontal lines, and a checker pattern. They performed their tests with aperture values of zero, three, and six. The vertical lines test is analogous to the horizontally adjacent pixel test (shown in the left columns of Figure 6) and the

	BVM-F250	PVM-2541
Red (cd/m^2)	34.7	33.3
Green (cd/m^2)	77.0	112.7
Blue (cd/m^2)	8.6	14.7
Red + green + blue (cd/m^2)	120.3	160.7
Percent difference from white	0.6	0.8

Table 2. Summary of spectral properties of each display in the native color mode.

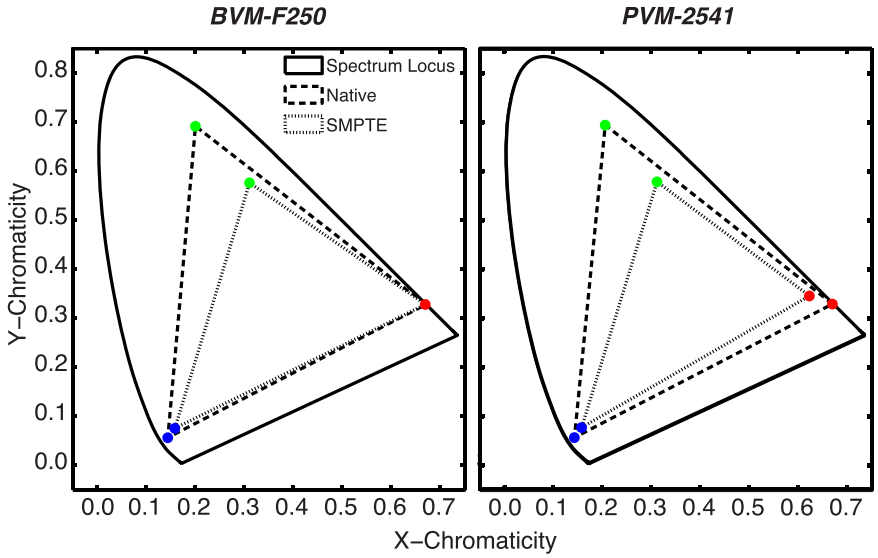

Figure 4. Color gamut of BVM and PVM OLED displays. Abscissa values indicate *X*-chromaticity. Ordinate values indicate *Y*-chromaticity, measured by the PhotoResearch PR 715 photometer. Solid line indicates the spectrum locus.

horizontal lines test is analogous to the vertically adjacent pixel test (shown in the right columns of Figure 6). However, the results reported here are for pixels illuminated to 60% of the maximum luminance, whereas in Ito et al. (2013) the vertical and horizontal lines were alternating between black (minimum luminance) and white (maximum luminance). The edge enhancement functionality of aperture is not measurable when adjacent pixels are alternating black and white, because contrast cannot be boosted any further. Predictably, the authors report only finding low-pass filtering (edge blurring) for vertical lines at aperture values of zero and three, and do not report the edge enhancement at a value of six. They also report that blurring is always present for horizontal lines, consistent with our findings. Based on this black/white line test, the authors recommend that an aperture value of six should be used. By performing our measurements with pixels at 60% of the maximum luminance, we were able to detect the edge enhancement that occurs at higher aperture values, suggesting that four would be a better setting to minimize pixel interactions. Note that this result may be specific to display input via DVI or Mini DisplayPort to HDMI, used in both studies. For other input sources (such as composite and SDI), an additional display control ("V Sharpness") is available, which might allow adjustment of vertical interactions.

	BVM-F250		PVM-2541	
	x	*y*	*x*	*y*
Red	0.670	0.328	0.670	0.329
Green	0.201	0.692	0.206	0.694
Blue	0.144	0.057	0.143	0.056

Table 3. Chromaticity *xy* coordinates of subpixels of each display in the native color mode.

Temporal precision

Figures 7 and 8 show the change in luminance over time for two cycles of a 5 Hz flickering stimulus and for one cycle of a 30 Hz flickering stimulus, respectively. In each case the display alternated between 97.5% and 2.5% of the maximum displayable

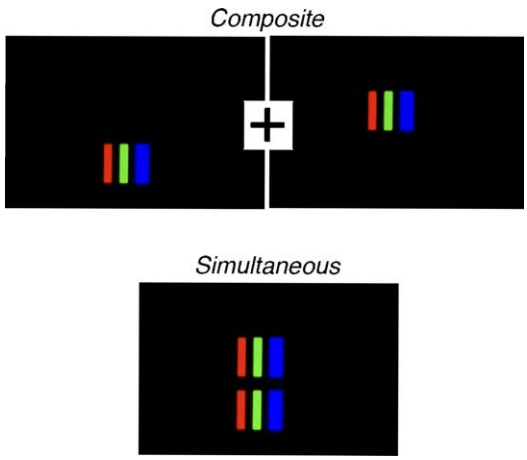

Figure 5. Pixel independence test. For each test, two adjacent pixels are illuminated separately and imaged by the Nikon D2Xs. These two images are linearly combined to create the *composite* image (upper panel). The composite is then compared to a single image taken with the same two pixels illuminated simultaneously (lower panel: *simultaneous*).

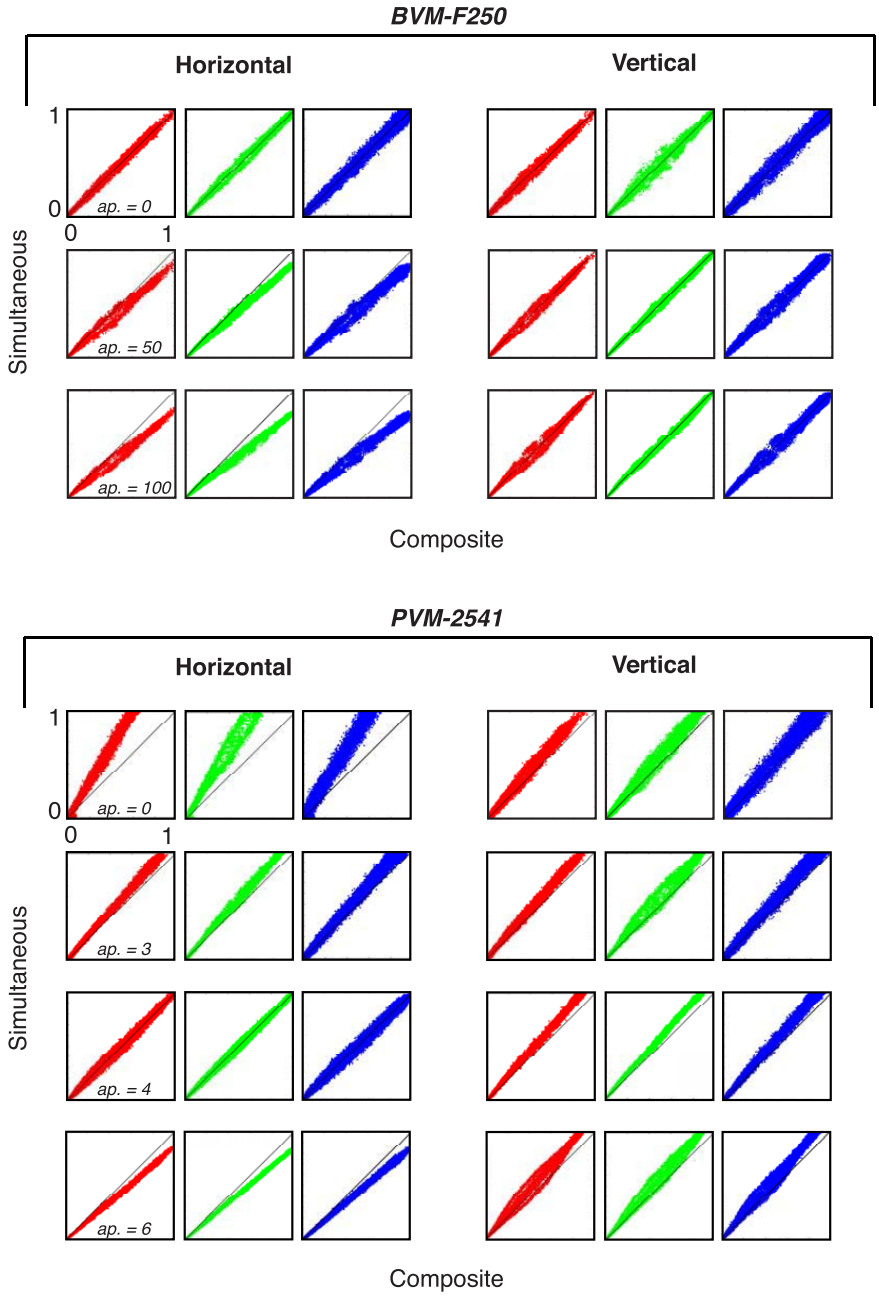

Figure 6. Pixel independence results for BVM and PVM OLED displays. Abscissa values indicate pixel intensity values from the composite images. Ordinate values indicate pixel intensity values from the simultaneous image. All values were measured with a Nikon D2Xs and converted to normalized arbitrary units. Data points colored red, green, and blue indicate values from the red, green, and blue channels of the camera images. The black lines indicate the identity line. The edge enhancement/blurring settings (referred to as aperture by the manufacturer) for each row are indicated in the initial panel. In order to keep axes the same across plots, some data points are not shown.

luminance and the refresh rate was 60 Hz. For comparison, each panel shows the results for a different display: the BVM and PVM OLEDs on the left (an additional panel shows the results with the PVM flicker free mode activated—120 Hz double flash), along with an HP P1230 CRT, an LG Flatron D2342 LCD, and a Dell U2410 LCD on the right. Note that the ordinate axis scale differs for each display. The BVM and PVM temporal responses reflect the fact that OLED pixels are fast-responding transducers: within a single 60 Hz frame, they rise to and fall from their active state quickly and only once, with a roughly 40% duty cycle. In the flicker free mode, the PVM behaves similarly but rises and falls

BVM-F250			PVM-2541		
Aperture	Horizontal	Vertical	Aperture	Horizontal	Vertical
0	1.00	1.00	0	2.70	1.32
50	0.77	1.00	3	1.31	1.32
100	0.65	0.99	4	1.00	1.33
			6	0.74	1.32

Table 4. Summary of pixel independence properties of each display. Independence is quantified as the slope of the best-fit regression line.

twice. The CRT shows a typical temporal response with a fast rise time and slightly slower decay. Because it has significantly less active time within a frame, each active interval is much brighter than the same interval on the OLEDs. The LCDs each exhibit multiple luminance modulations within a single frame. These modulations are presumably due to the flicker of the backlights on the LCDs (Elze & Tanner, 2012). Backlight modulations can be very fast and have a symmetric temporal profile because they are not constrained by the opening and closing of the LCD pixels, but rather produced by a panel often composed of light emitting diodes or fluorescent lights. The LG Flatron D2342 backlight modulates the display luminance at 240 Hz, with very low minimum luminance (visible in the sharp notches in middle right panel of Figure 8). The Dell U2410 backlight modulation is of a lower magnitude and occurs at 180 Hz.

Examples of rise-time and fall-time were taken from the data used to plot Figure 8 and are reported in Table 5. Time 0 was taken as the first data sample before a light increase was measurable and the rise-time was specified as the time it took for the luminance to reach 90% of the maximum light output reached when alternating at 30 Hz. Fall-time was measured from the last sample at the maximum luminance until light output fell to within 10% of the minimum displayed luminance level (ignoring backlight modulations on the LCDs). The temporal characteristics reported here for the PVM are in good agreement with the measurements from Ito et al. (2013). Note that these durations do not take into account any processing delay in the displays.

Discussion

Luminance

Both OLED display models have large contrast ratios compared to typical contrasts used in visual experiments (e.g., Kihara et al., 2010; Legge & Foley, 1980; Robson, 1966; Stone & Thompson, 1992). The measured contrast ratios were comparable to typical CRT ratios and larger

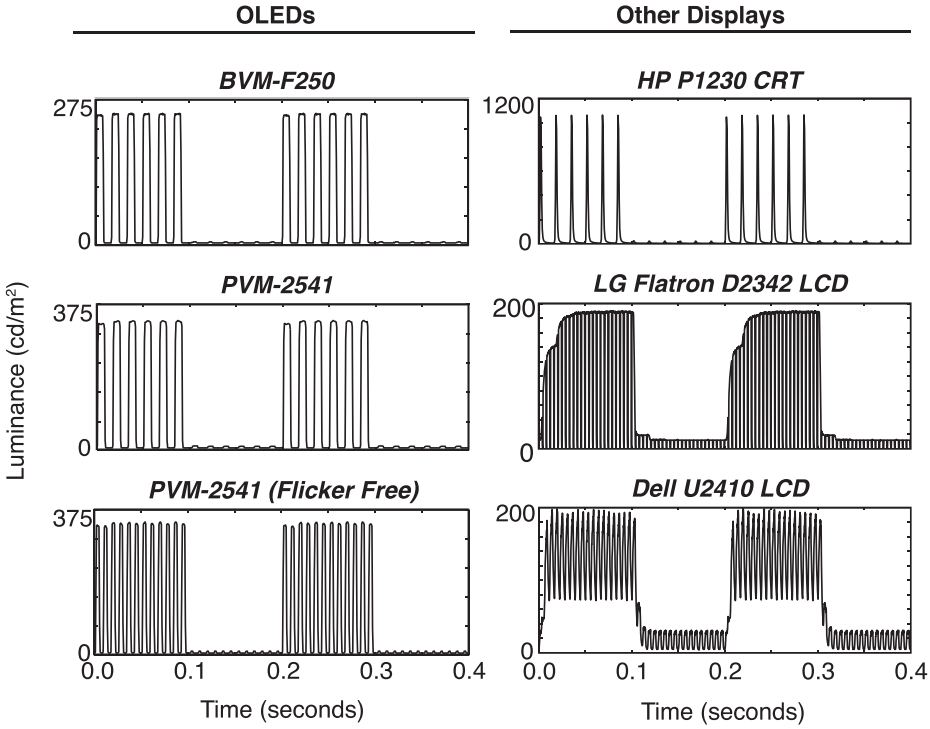

Figure 7. Temporal profiles of the BVM and PVM OLED displays compared with the CRT and LCD displays. Abscissa shows time in seconds. Ordinate values indicate the display luminance measured by the photodiode, and the ordinate axes are scaled differently for each display. The stimulus was an alternation between 97.5% and 2.5% luminance at 5 Hz.

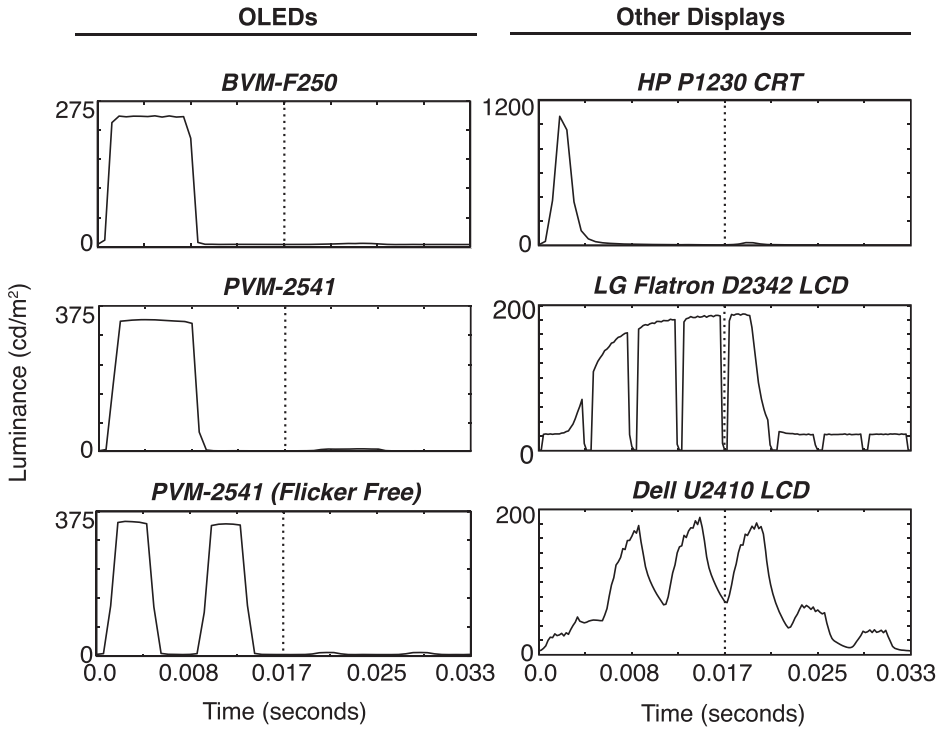

Figure 8. Additional temporal profiles for a single contrast reversal at 30 Hz. Each panel shows two 60 Hz frames: one 97.5% luminance, followed by 2.5% luminance. Dashed vertical lines indicate the duration equal to a single frame (0.0167 s). However, note that these plots do not show the processing delay of the displays: Time Point 0 is the first data sample before a measureable light increase.

than typical for LCDs (Gaylord, 2006). Because the OLED display panels have self-emitting pixels and do not have the backlights of LCDs or the phosphor flare of CRTs, the achievable contrast ratio is theoretically significantly higher than these other displays. The effective contrast ratio is likely limited by surrounding ambient light more than any residual light emission from the OLED pixels (in other words, OLEDs have a black black). The gamma correction of the displays can be well fit by power functions if the proper display settings are used; the displays can therefore be easily linearized for luminance. However, when selecting brightness and contrast settings, care must be taken to prevent overpowering the displays, which leads to a saturation in the higher luminance values, and to prevent setting the brightness too low, which leads to deviations from a well-behaved power function. The bit value at which the luminance saturates can be dependent on the amount of the display being illuminated (also see Ito et al., 2013).

Spectrum

The spectral measurements show that channel independence holds for both PVM and BVM models. This means that there are no noticeable interactions between RGB channels. As a consequence, one can easily calculate the spectrum for any color as a linear combination of the red, green, and blue spectrum. Compared to typical CRT and LCD displays, both PVM and BVM OLED models show a well-shaped RGB spectrum in native mode (Chiu & Lee, 2010; Sharma, 2002). The OLED spectra are much more narrow-banded and isolated, which can lead to a much larger color gamut. The measured color gamut is larger than the widely used sRGB (Anderson, Motta, Chandrasekar, & Stokes, 1996) and Adobe RGB color space (http://www.adobe.com/digitalimag/adobergb.html). Nevertheless, one must still consider how to map color values that are outside of this larger color gamut.

	Rise time (ms)	Fall time (ms)
BVM-F250 OLED	1.3	1.3
PVM-2541 OLED	1.9	1.3
HP 1230 CRT	1.9	2.6
LG Flatron D2342 LCD	8.9	3.2
Dell U2410 LCD	8.9	6.1

Table 5. Summary of temporal precision transitioning between 97.5% and 2.5% luminance at 30 Hz. Rise and fall times were calculated from the data in Figure 8. Rise time indicates the delay to reach luminance at 90% of the maximum. Fall time indicates the delay to reach luminance within 10% of the minimum.

To create the SMPTE color modes, one must illuminate both red and green OLED pixels to create a new green primary. This new green primary is closer to the white point and shrinks the color gamut relative to the native color display gamut. This option is available, however, if one would like to strictly adhere to the SMPTE-C standard and thus simulate color for CRTs, or broadcast programs in North America.

Pixel independence

Interactions between adjacent pixels on a display can cause differences between the desired and displayed luminance. Limitations in CRT circuitry can lead to interactions between horizontal pixels, whereas LCDs do not suffer from the same limitations (Farrell et al., 2008). Both OLED display models allow adjustment of pixel independence via a control referred to as *aperture correction*. Aperture correction is an implementation of edge enhancement designed to boost the spatial contrast in a displayed image (Hagerman, 1993). In the case of the OLEDs, the BVM model had excellent horizontal and vertical pixel independence when aperture was disabled. Increasing the aperture parameter resulted in pixel interactions one would expect to see with edge enhancement. The PVM model does not have an option to completely disable aperture when the display input comes from a computer via HDMI, but there are settings that produce predicable pixel interactions comparable to those on a CRT display (see figures 7 and 8 in Farrell et al., 2008). Such interactions should only be a limitation for visual stimuli where contrast must be modulated at very high spatial frequencies with high precision. Also, because these interactions (a) are not likely inherent to the display hardware and (b) are predictable, it should be possible to calculate the expected pixel interactions based on proximity and luminance, and adjust pixel values in order to undo the effects of aperture in some cases.

Pixel independence measurements were conducted on pairs of adjacent pixels; however, the largest aperture settings on the BVM introduced clear interactions beyond just the neighboring pixels. In most cases, the aperture settings used will be the ones that minimize pixel interactions, in which cases the interactions appeared to be essentially limited to adjacent pixels.

Temporal precision

The rise and fall times of the OLED displays were faster than the CRT and LCD models tested (except the PVM rise time, which was similar to the CRT). They were also more symmetric: the CRT had a longer off-tail than the OLEDs, and the LCDs had slower and highly asymmetric rise and fall times. These results indicate that OLED displays are a suitable replacement for CRTs for clinical electrophysiology laboratories that wish to adhere to the International Society for Clinical Electrophysiology of Vision (ISCEV) standard for pattern visually evoked potentials (VEPs) and electroretinograms (ERGs) (http://www.iscev.org/standards). LCD displays are unsuitable for generating pattern reversal stimuli because of their asymmetric opening and closing times. The asymmetry causes a time-varying change in the mean luminance that creates a luminance artifact in what is supposed to be a pure pattern response.

The rapid on-off switching of the OLED pixels leads to visible flicker at the 60 Hz refresh rate. This flicker can be significantly reduced in two ways: the BVM can be driven with 72 and 75 Hz triple flashed frames (content updates at 24 or 25 Hz) with each frame shown three times, and the PVM flicker free mode drives the display at 120 Hz (content still updates at 60 Hz, but each frame is shown twice).

The processing delay (i.e., the time between when a signal is sent to the display and when it is actually displayed on the screen) was not assessed in the current measurements. To determine the usability of the BVM and PVM for research applications that require minimal processing delays, additional measurements will be necessary.

Estimating the light properties produced by displays

Using the data from the display measurements reported here, we have provided a MATLAB tutorial for estimating the luminance and radiance produced by any image on these two OLED displays, and for comparing these results to an example CRT and LCD. This tutorial relies on the display simulation functionality of the Image System Engineering Toolbox for Biology (ISETBIO), a MATLAB toolbox (Wandell, Winawer, Brainard, Hofer, & Farrell, 2013). The tutorial and associated files can be downloaded from https://github.com/eacooper/OLED_RGB2Radiance and are also available as supplemental files with this report. The tutorial loads in digital display values and produces an estimate of the image luminance and radiance emitted by the BVM and PVM displays, as well as an example CRT and LCD. The estimates produced by the script assume that display settings and properties match those described in this report, with the exception that for these simulations spatial pixel independence is assumed. This assumption should hold for the BVM, and should be a good estimate for the PVM when the spatial frequencies in the image are not

predominated by the highest displayable frequency (high contrast between adjacent pixels). Also, due to the fast temporal responses of both OLED displays, estimates of radiance and luminance for images produced sequentially on these displays should be applicable (i.e., temporal independence should also hold, allowing for the prediction of changes in light over time as well as space).

Other considerations

All of the reported display properties were measured with devices aimed directly in front of the displays. We did not formally test the effect of off-axis viewing angle on display luminance and chromaticity. Detailed measurements of luminance and chromaticity changes caused by off-axis viewing for the PVM model are reported in Ito et al. (2013) and agree with our informal assessments. These results show that luminance decreases and chromaticity shifts towards cyan with increasingly steep viewing angles. The magnitude of the shift is similar to or smaller than those measured on an example CRT and LCD (Ito et al., 2013). The second-generation models of both the PVM and BVM displays, which are currently available, have been designed to improve off-axis image quality.

Increasing display lifetime (duration to half-brightness) to a usable level for consumer displays has been a challenge for developing OLED displays, particularly for blue subpixels (Geffroy et al., 2006). A relatively shorter lifetime for blue could lead to a red shift in the displays over time. Ito et al. (2013) report no change in luminance or chromaticity in the PVM model after four months of usage; however, this is still a relatively short period of time compared to the desired lifetime for a laboratory display. Documentation from Sony reports that the duration to half-brightness of their OLED displays is approximately 30,000 hr, and that internal sensors help to minimize red-shift over time (http://www.avcom.tv/Galleries/ShowFile.aspx?id=273). Testing these claims was beyond the scope of the current study.

Conclusions

Current commercially available OLED displays are capable of producing visual stimuli appropriate for a wide-range of vision research applications. Their extremely dark black level, wide color gamut, and rapid and symmetric temporal response make them a viable option to replace CRTs and LCD displays for demanding vision research experiments.

Keywords: display characterization, spatio-temporal precision, spectrum, OLED, stimulus presentation

Acknowledgments

The OLED monitors were donated to Stanford University by SONY Corporation. EAC was supported under a research contract between SONY and Stanford University. AMN and VV were supported by NIH grants 2R01EY018875-04A1 and 2R01EY015790-06A2.

Commercial relationships: Yes.
Corresponding author: Emily A. Cooper.
Email: eacooper@stanford.edu.
Address: Department of Psychology, Stanford University, Stanford, CA, USA.

References

Anderson, M., Motta, R., Chandrasekar, S., & Stokes, M. (1996). Proposal for a standard default color space for the Internet: sRGB. *Proceedings of IS&T/SID 4th Color Imaging Conference* (pp. 238–245). Scottsdale, AZ.

Bach, M., Meigen, T., & Strasburger, H. (1997). Raster-scan cathode-ray tubes for vision research—Limits of resolution in space, time and intensity, and some solutions. *Spatial Vision, 10*(4), 403–414.

Brainard, D. H. (1989). Calibration of a computer controlled color monitor. *Color Research & Application*, *14*(1), 23–34.

Brainard, D. H. (1997). The Psychophysics Toolbox. *Spatial Vision, 10*(4), 433–436.

Brainard, D. H., Pelli, D. G., & Robson, T. (2002). Display characterization. In J. Hornak. (Ed.), *Encyclopedia of imaging science and technology* (pp. 172–188). New York, NY: Wiley.

Chiu, T.-L., & Lee, J.-H. (2010). Color gamut variation of LED-lit LCD at different module temperatures. *Optics Communications, 283,* 373–378.

Cowan, W. (1995). Displays for vision research. In M. Bass (Ed.), *Handbook of optics, volume 1: Fundamentals, techniques, and design* (pp. 27.1–27.44). New York, NY: McGraw-Hill.

Elze, T., & Tanner, T. G. (2012). Temporal properties of liquid crystal displays: Implications for vision science experiments. *PLoS One, 7*(9), e44048.

Farrell, J., Ng, G., Ding, X., Larson, K., & Wandell, B. (2008). A display simulation toolbox for image

quality evaluation. *Journal of Display Technology*, *4*(2), 262–270.

García-Pérez, M. A., & Peli, E. (2001). Luminance artifacts of cathode-ray tube displays for vision research. *Spatial Vision, 14*(2), 201–15.

Gaylord, P. (2006). Issues in defense training systems immersive displays. *Proceedings of SPIE, 6225,* 62250O–1–62250O–12.

Geffroy, B., le Roy, P., & Prat, C. (2006). Organic light-emitting diode (OLED) technology: Materials, devices and display technologies. *Polymer International*, *55*(6), 572–582.

Hagerman, J. (1993). *Some notes on aperture correction.* Carlsbad, CA: Hughes-JVC Technology Corp. Retrieved from http://www.hagtech.com/pdf/aperture.pdf.

Ito, H., Ogawa, M., & Sunaga, S. (2013). Evaluation of an organic light-emitting diode display for precise visual stimulation. *Journal of Vision*, *13*(7):6, 1–21, http://www.journalofvision.org/content/13/7/6, doi:10.1167/13.7.6. [PubMed] [Article]

Kihara, K., Kawahara, J., & Takeda, Y. (2010). Usability of liquid crystal displays for research in the temporal characteristics of perception and attention. *Behavior Research Methods, 42*(4), 1105–1113.

Kleiner, M., Brainard, D., & Pelli, D. (2007). What's new in Psychtoolbox-3? *Perception, 36*(14) (ECVP Abstract Supplement).

Lagroix, H. E. P., Yanko, M. R., & Spalek, T. M. (2012). LCDs are better: Psychophysical and photometric estimates of the temporal characteristics of CRT and LCD monitors. *Attention, Perception & Psychophysics, 74*(5), 1033–1041.

Lee, E., & Song, J. (2012). High efficiency organic light-emitting display using selective spectral photorecycling. *Applied Physics A: Materials Science & Processing*, *109*(2), 431–436.

Lee, B. M., Yu, H. H., Kim, Y. H., Kim, N. H., Yoon, J. A., Kim, W. Y., ... Mascher, P. (2013). Highly efficient blue organic light-emitting diodes using dual emissive layers with host-dopant system. *Journal of Photonics for Energy*, *3*(1), 1–9.

Legge, G. E., & Foley, J. M. (1980). Contrast masking in human vision. *Journal of the Optical Society of America, 70*(12), 1458–1471.

Lyons, N. P., & Farrell, J. E. (1989). Linear systems analysis of CRT displays. *SID Digest, 10,* 220–223.

Pardo, P. J., Pérez, A. L., & Suero, M. I. (2004). Validity of TFT-LCD displays for colour vision deficiency research and diagnosis. *Displays*, *25*(4), 159–163.

Pelli, D. G. (1997). The VideoToolbox software for visual psychophysics: Transforming numbers into movies. *Spatial Vision, 10*(4), 437–442.

Robson, J. G. (1966). Spatial and temporal contrast-sensitivity functions of the visual system. *Journal of the Optical Society of America, 56*(8), 1141–1142.

Sharma, G. (2002). LCDs versus CRTs—Color-calibration and gamut considerations. *Proceedings of the IEEE, 90*(4), 605–622.

Singh, R., Narayanan Unni, K. N., & Solanki, A. (2012). Improving the contrast ratio of OLED displays: An analysis of various techniques. *Optical Materials*, *34*(4), 716–723.

Sperling, G. (1971). The description and luminous calibration of cathode ray oscilloscope visual displays. *Behavioral Research Methods & Instruments*, *3*(3), 148–151.

Stone, L. S., & Thompson, P. (1992). Human speed perception is contrast dependent. *Vision Research, 32*(8), 1535–1549.

Wandell, B. A., Winawer, J., Brainard, D. H., Hofer, H., & Farrell, J. E. (2013). *isetBio: Integrated tools for modeling visual encoding and early visual system processing*. Retrieved from https://github.com/isetbio.

Watson, A. B. (2010). Display motion blur: Comparison of measurement methods. *Journal of the SID, 18*(2), 179–190.